HYSTERESIS BEHAVIOR OF THREE STORY CONCENTRIC K-BRACED FRAMES

T. FUKUTA (1)
H. YAMANOUCHI (2)
I. NISHIYAMA (3)
N. ENDOH (4)
T. WATANABE (5)
Presenting Author: T. Fukuta

SUMMARY

The restoring force characteristics of the planar steel braced frames are clarified by a series of the cyclic loading experiment and some analyses. It is one of the Japanese side supporting tests on the full-scale seismic tests of the six-storied steel building conducted under the U.S.-Japan Co-operative Research Program Utilizing Large-Scale Testing Facilities. The test frames were modeled to be the lower part of the high-rise building with concentric K-type braces. Some part of the test results and analyses are presented in this paper.

INTRODUCTION

Many experimental and analytical works have been carried out on the post yielding behavior of structural steel members, and their structural behavior has been gradually made clear, but the over-all behavior of the frames with concentric K-braces has not been yet clear. So the authors tested and analyzed the frames as shown in Fig. 1 in order to evaluate the relationship between strength and ductility of each member, and to estimate the effects of braces and other members on the over-all behavior of the frames.

EXPERIMENTS

Test Specimens

Specimens consisted of two braced frames with the composite beams, three bare frames with braces, and one bare frame without braces. Each specimen had two identical planar frames in the loading direction, not to cause the out-of-plane deformation. The third story was used mainly for loading.

ASTM A36 structural steel was used for the beams and columns. The width-to-thickness ratios of these members were limited to the structural ranks FA or FB in Japanese Seismic Design Code. The beam-to-column connections should be designed to be moment connections in the loading direction and to be shear

(1) Research Engineer, International Institute of Seismology and Earthquake Engineering, Building Research Institute (B.R.I.), Japan

(2) Head of Structure Division, B.R.I.

(3) Research Engineer, Structure Division, B.R.I.

(4) Structure Engineer, Toda General Contractor Co.

(5) Structure Engineer, Maeda General Contractor Co.

connections in the transverse direction. The slenderness ratios of the beams around the weak axis should be less than 170.

The braces were designed to resist both tensile and compressive forces and had built-up box sections so that buckling should be confined to the plane of the frame. JIS SS41 structural steel was used for these braces.

The beams of Specimen No.1 and No.2 were designed to act compositely by the headed studs with 70mm length and 16mm diameter and steel decks with 1.2mm thickness. Light-weight concrete was in use for slabs. Its specified compressive strength was 270kg/cm^2 and slamp was 18cm. The artificial light-weight coarse aggregate and sand for fine aggregate were used. Objectives of these specimens are to evaluate the effects of the composite beams and braces on theover-all behavior of the frames, in comparison with the results of Specimens No.3 and No.4, and to gain the effects of asymmetric framing on the restoring characteristics by applying the different loading programs respectively. Specimen No.3 is a bare frame without braces, designed to estimate the contributions of the moment frame action to the over-all braced frame behavior in comparison with Specimens No.1 and No.2. Specimen No.5 and No.6 had different size braces, beams, and columns from the other specimens.

Loading Program

The elastic and plastic response of the full-scale test specimen, which is the prototype building of Specimen No.1, was analyzed using the Miyagiken-oki earthquake of 1978. In this analysis the axial forces in the columns reached to 50-70 percent of the axial yield strength of the columns. Such high axial forces would affect the over-all behavior of the structure. Therefore, in this test, the vertical forces were applied to the specimens, corresponding to the horizontal force. To determine the relationship between these forces, the elasto-plastic frame analysis was carried out on the full-scale test specimen. According to this analysis, it was found that the relationship was almost linear through the entire stress range. Thus, the axial forces in the columnsand lateral forces were always applied to maintain the linear relationship in this test. For example, Fig. 3 shows the actually applied forces to Specimen No.1.

The distribution beam of loads was fixed at the top floor level of the specimens. The horizontal forces to the specimens were the cosine component of the forces of the inclined actuators controlled by the digital displasement transducers. The vertical forces were totals of the sine components of the actuator forces and the center-hole jack forces applied vertically. The bases of the columns were fixed to the floor beams connected to the testing bed not to move laterally (see Fig. 2).

Properties of Materials

Table 2 shows the results of tensile tests for the used steels, and Table 3 gives the results of compressive and splitting tensile tests for the concrete.

HYSTERESIS BEHAVIOR OF K-BRACED FRAMES

The braces were buckled at the drift angle between 1/300 and 1/400 radian in Specimens No.1 and No.4 (see Fig. 4). This was just an early stage of the lateral deformation of the frames. After the buckling of the braces, the

specimens lost only a few percent of its resisting shear forces. Specimen No.4 had no gain of the resisting shear forces in the cyclic loading after the buckling of braces. In case of Specimen No.1, the further deformation gained the maximum strength, when the drift angle was 1/70 radian. This could be explained by the composite effects of concrete floor slabs on the strength of beams. The calculated full plastic moment of beams in Specimen No.1 was 2.42 times those in Specimen No.4 for positive bending and 1.34 times for negative bending. Specimen No.1 was found to have a higher shear capacity in the moment frame than the bare braced frame. The midspans of the beams in the braced bay were pull down by the tension-side braces after the buckling of braces. However the concrete floor slabs restrained these downward deformations better better than in case of Specimen No.4 (see Fig. 5). The better restraintment by the concrete slabs caused the tension-side braces to carry high axial forces. In case of Specimen No.1, the axial forces of tension-side braces reached to the axial yield strength of braces, on the contrary, the braces of Specimen No.4 did not experience the axial yield strength (see Fig. 6). Specimen No.1 had the very ductile load-deformation relation. This specimen kept 90 percent of its maximum strength at the 1/25 drift angle.

Behavior of Braces

The definition of K-factors of braces are given from the following equation.

$$Qb=2Nb\cos\theta$$
$$Nb=Ny(1-0.4\lambda^2/\Lambda^2) \qquad (1)$$
$$K=L/Lg$$
$$L=\lambda i$$

where
- Qb : shear force carried by braces at the buckling of braces
- Nb : axial force of braces
- Ny : axial yield strength of braces
- Lg : inside measurement of gusset to gusset
- λ : effective slenderness ratio
- Λ : critical slenderness ratio
- i : radius of gyration of area of the brace

K-factors by this way are almost equal to 1.0, i.e. the effective length of braces for buckling is about inside measurement of gusset to gusset and Specimen No.4 has the same K-factors of braces as Specimen No.1. This shows that against the buckling of braces there is no difference between the steel beams and the composite beams with such dimensions as Specimens No.1 and No.4.

The axial forces of braces are calculated from the data of the strain gauges attached to the braces by the following assumptions; (a) stress-strain relation of the steel material is represented by the three straight lines which imply the elastic part, the strain hardening one and the softened one due to the Bauschinger effect, and (b) the section of the braces are divided into four parts, two flanges and two webs, and each part of the section has the above-mentioned tri-linear stress-strain relation.

Fig. 7 shows the calculated axial force and the measured axial displacement relation of the braces of Specimens No.1 and No.4. The solid line in Fig. 8 is the shear force carried by the braces gained by this way. The dotted line shows the value Qb= Qtotal-Qc, where Qtotal is horizontal force, and Qc is sum of the shear forces in columns gained by the data of the strain gauges. This implies that the axial forces of braces are adequately given by the above mentioned way. The dotted lines in Fig. 7 are the analytical solu-

tions of the pin-supported column which is applied by axial forces. The main assumptions of this analysis are the followings: (a) after the buckling, the midspan of the brace is deformed to the transverse direction and behaves as a plastic hinge. (b) the stress-strain relation is elasto-plastic at the plastic hinge and the rest of the member elastic. (c) the yield function of the member is parabola. It is found that the falling branch of the load-displacement curve of these braces could correspond to the analytical results of the brace with the slenderness ratio 50 to 65.

Damage of Specimens

Fig. 4 shows the damage of the specimens at the final stage. In Specimens No.1 and No.4, the damage concentrated in the first and second story. On the other hand, the damage was distributed almost equally to each story in Specimen No.3. The braces had three plastic hinges at midspan and the both ends. The flanges and webs at the plastic hinges were locally buckled and some of them were ruptured because of the low-cycle and high-stressed loading. In the braced frames, the M and N columns (see Fig. 1) were more severely damaged than the S columns. At the first story, the maximum axial forces in the M and N columns were 0.53Ny to 0.77Ny and in case of the S columns at most 0.2Ny to 0.25Ny. Ny is the yield axial strength of the columns. The beams in the braced bay were pull down at their midspans by the tension-side braces and widely damaged by the bending moments and axial forces. In case of Specimen No.1, concrete floor slabs around the beam-to-braces connections were finally separated from the steel beams, and the beams lost the composite effect on their strength.

PREDICTION ON RESTORING SHEAR FORCES OF K-BRACED FRAMES

The restoring force characteristics of the test structure are estimated by means of the following procedures. (a) In this analysis, the braced frame is parted into the moment frame and the brace component as shown in Fig. 9. (b) The moment frame has the elasto-plastic load-deformation relation produced by the stocky beams and columns. The ultimate shear capacity of the moment frame is calculated by the virtual work method. (c) The brace component is composed of the braces and beams supported with the pins. (d) The buckling strength of the compression-side brace is refered to the test results In the post-buckling range, the K-factor is 0.5, because its post-buckling branch of the axial force and the axial displacement curve is similar to those of the member which has 0.5 K-factor and the specimen had finally three hinges in braces. (e) The resisting shear force of the tension-side brace is calculated in consideration of the downward deformation of the beam-to-braces connection and the strength of the beams. (f) The restoring shear force of the braced frame is evaluated by the following equation;

$$Qu(x)=Qr(x)+cQb(x)+tQb(x) \qquad (2)$$

Qu(x) : restoring shear force of the structure
Qr(x) : restoring shear force of the moment frame
cQb(x) : restoring shear force of the compression-side brace ($=\alpha Ny\cos\theta$)
tQb(x) : restoring shear force of the tension-side brace
($=\alpha Ny\cos\theta$:in elastic range,
$=\alpha Ny\cos\theta + Pby\cot\theta$:in post-buckling range)
Pby : shear strength of the beam in the braced bay ($= 2Mpb/Lb$)
Mpb : full plastic moment of the beam in the braced bay
Lb : half of the span length of the beam in the braced bay

α : ratio of the axial force to the axial yield strength of the brace

x : story drift deformation of the structure

Qr(x), cQb(x) and tQb(x) are drawn in Fig. 10. Fig. 11 shows the results of this analysis and the experiment. The analytical curve of Specimen No.1 is in overestimation to the test results. This specimen lost the composite effect of the concrete floor slabs on the strength of the beam at the largely deformed stage (see chapter Damage of Specimens). If Mpb in tQb(x) is assumed to be the full plastic moment of the steel beam instead of the composite beam, Qu(x) after the buckling of braces is 8.7ton less than the value drawn in Fig. 10.

CONCLUDING REMARKS

The three story planar frames with concentric K-braces, which are the lower part of the high-rise steel building, are investigated to gain the restoring force characteristics.

Test results indicate that the specimen with the composite beams has the very ductile load-deformation relation.

The K-factor of the braces for the buckling is about 1.0, assuming that the effective length of braces is inside measurement of gusset to gusset. The falling branch of the axial force-axial displacement relation of the braces in the frames would correspond to that of the members with the K-factor about 0.5 to 0.65.

A good approximation of the over-all restoring force characteristics of these structures could be obtained by the presented analysis. The strength of the beams in the braced bay and the post-buckling behavior of the compression-side braces would be the important factors in this analysis.

REFERENCES

1)Fukuta,T., Yamanouchi,H., and et al. : Full-Scale Seismic Tests of a Steel Building and the Supporting Tests on its Half-Scaled Partial Frames,15th Joint Meeting U.S. Japan Panel on Wind and Seismic Effects,U.J.N.R.,May 1983

2)Watabe,M.,Ishiyama,Y. :Earthquake Resistant Regulations for Building Structures in Japan,Earthquake Resistant Regulations A World List,1980

3)Yamada,M.,Tsuji,B.:Bauschinger Model, Summary of the Technical Report of the Annual Meeting of the A.I.J.,Aug. 1973

4)Takanashi,K.,Yamada,T. :Modelization for the Elasto-Plastic Analysis of Braces,Summary of the Technical Report of the Annual Meeting of the A.I.J., Sep. 1976

Table 1 Member sizes of specimens

	Specimen 1&2	3	4	5	6
N&S-column 1-fl. - 3-fl.	6WF20	6WF20	6WF20	6WF20	5WF15
M-column 2-fl. & 3-fl.	6WF25	6WF25	6WF25	6WF25	6WF20
M-column 1-fl.	8WF35	8WF35	8WF35	8WF35	6WF20
beam 3-fl.	8WF10	8WF10	8WF10	8WF10	8WF13
beam 2-fl.	8WF13	8WF13	8WF13	8WF13	10WF17
brace 2-fl. & 3-fl.	box-105x45 x4.5	-	box-105x45 x4.5	box-70x35 x6	box-105x45 x4.5
brace 1-fl.	box-110x55 x4.5	-	box-110x55 x4.5	box-70x40 x9	box-110x55 x4.5
(unit;mm)					

Table 2 Mechanical properties of steel

	σ_y (ton/cm^2)		σ_{max} (ton/cm^2)		elongation (%)	
	flange	web	flange	web	flange	web
8WF35	2.75	3.39	4.44	4.67	28.9	22.5
8WF13	2.83	3.90	4.26	4.85	25.1	16.4
8WF10	3.13	4.58	4.14	5.18	20.2	10.3
6WF25	3.23	3.55	4.75	4.98	27.3	20.9
6WF20	3.47	4.12	4.89	5.36	25.2	17.8
5WF16	2.99	3.62	4.50	4.81	25.2	20.4
10WF17	2.89	4.04	4.50	5.01	26.5	18.4
E-4.5	2.78		4.14		32.7	
6.0	3.76		4.83		19.4	
9.0	3.17		4.53		27.4	
Bar ø6	4.54		6.71		21.5	

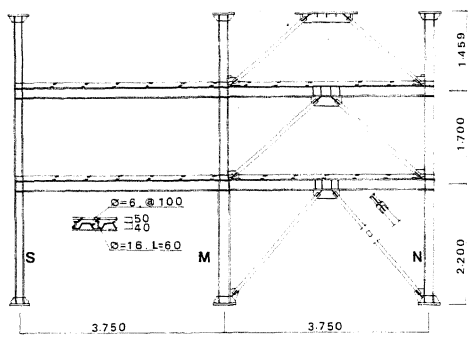

Fig. 1 Specimen No.1

Table 3 Mechanical properties of concrete

Specimen	T	Fc	Fst	Ec	$c\varepsilon_b$
No.1	1	287.0	22.9	265	0.170
	2	301.4	22.5	268	0.159

T = 1 before test
2 after test
Fc = compressive strength (kg/cm^2)
Fst = splitting tensile strength (kg/cm^2)
Ec = Young's modulus (ton/cm^2)
$c\varepsilon_b$ = strain at stress=Fc (%)

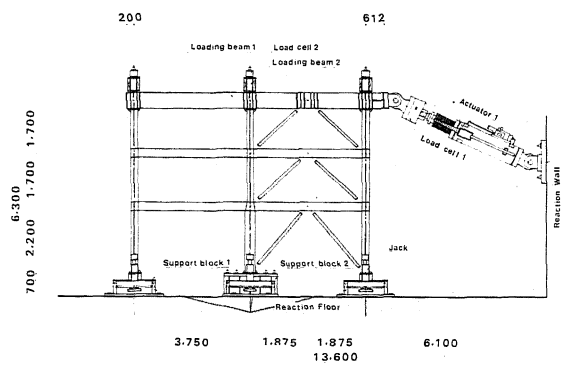

Fig. 2 Test set up

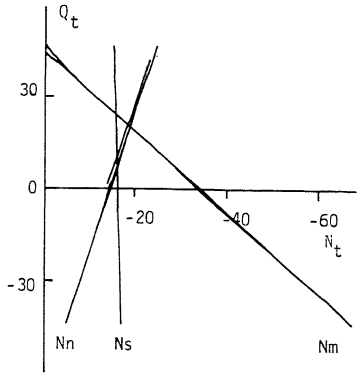

Fig. 3 Q-N relation applied to Specimen No.1

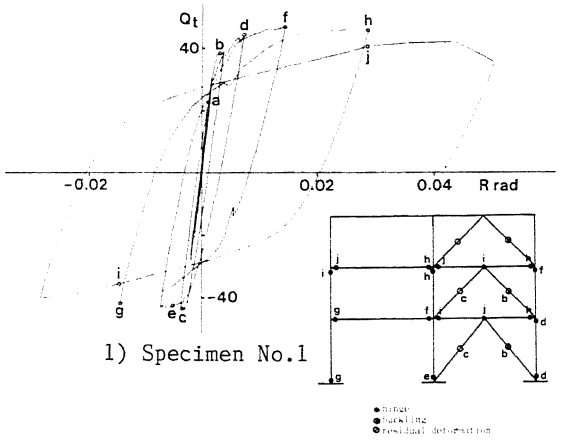

1) Specimen No.1

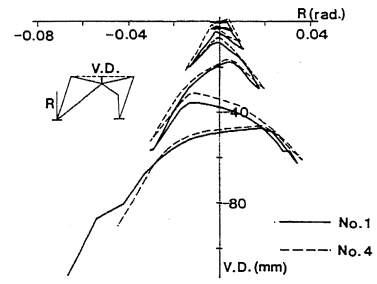

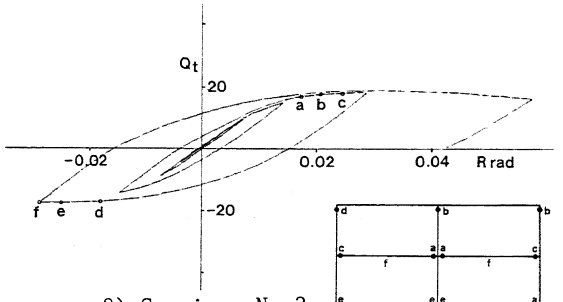

2) Specimen No.3

Fig. 5 Story drift angle - vertical displacement of the beam to brace connection (2-story)

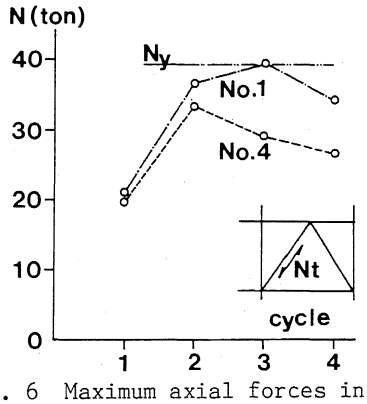

Fig. 6 Maximum axial forces in the tension-side braces at each loading cycle (1-story)

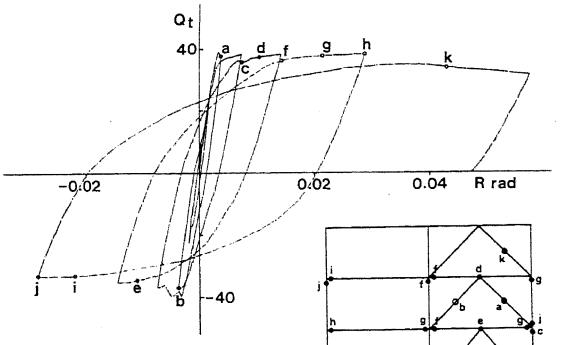

3) Specimen No.4

Fig. 4 Horizontal force - drift angle relation and final damage

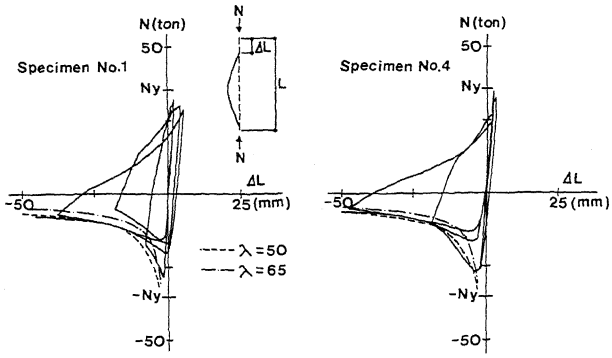

Fig. 7 Axial force and axial displacement of braces

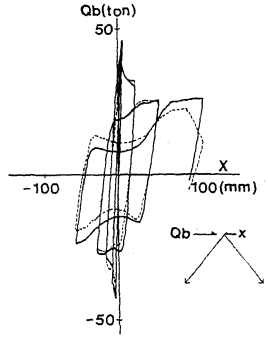

Fig. 8 Shear force carried by braces Specimen No.1 (2-story)

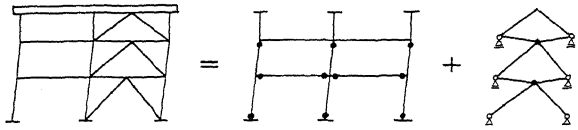

Fig. 9 Modelization for the analysis

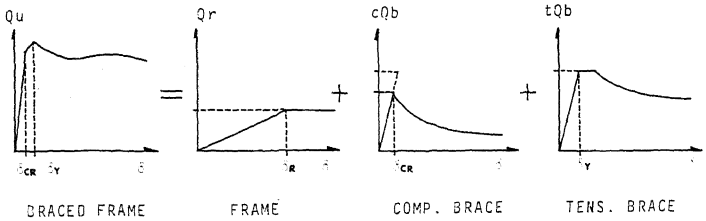

Fig.10 Restoring shear force of each component

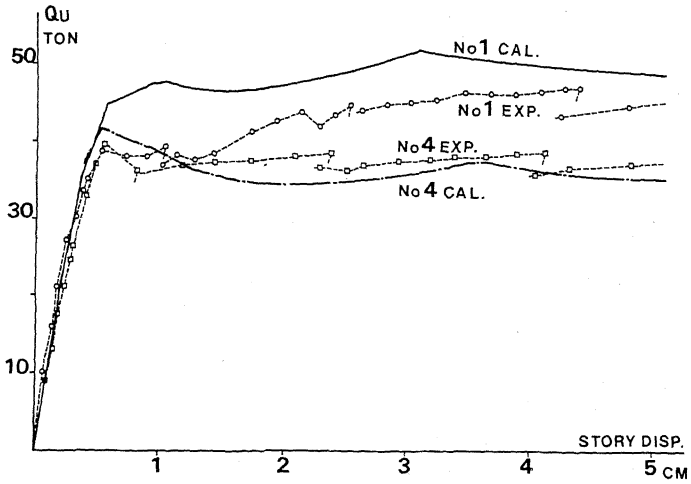

Fig.11 Restoring shear force of the structure (experiment and analysis)